



Landi, D., King, L., Zhao, Q., Rayfield, E. J., & Benton, M. J. (2021). Testing for a dietary shift in the Early Cretaceous ceratopsian dinosaur *Psittacosaurus lujiatunensis*. *Palaeontology*, 64(3), 371-384. <https://doi.org/10.1111/pala.12529>

Publisher's PDF, also known as Version of record

License (if available):  
CC BY

Link to published version (if available):  
[10.1111/pala.12529](https://doi.org/10.1111/pala.12529)

[Link to publication record in Explore Bristol Research](#)  
PDF-document

This is the final published version of the article (version of record). It first appeared online via Wiley at <https://onlinelibrary.wiley.com/doi/full/10.1111/pala.12529> . Please refer to any applicable terms of use of the publisher.

## University of Bristol - Explore Bristol Research

### General rights

This document is made available in accordance with publisher policies. Please cite only the published version using the reference above. Full terms of use are available: <http://www.bristol.ac.uk/red/research-policy/pure/user-guides/ebr-terms/>

# TESTING FOR A DIETARY SHIFT IN THE EARLY CRETACEOUS CERATOPSID DINOSAUR *PSITTACOSAURUS LUJIATUNENSIS*

by DAMIANO LANDI<sup>1</sup> , LOGAN KING<sup>1</sup> , QI ZHAO<sup>1,2</sup> ,  
EMILY J. RAYFIELD<sup>1</sup>  and MICHAEL J. BENTON<sup>1</sup> 

<sup>1</sup>School of Earth Sciences, University of Bristol, Queens Road, Bristol BS8 1RJ, UK; logan.king@bristol.ac.uk

<sup>2</sup>Institute of Vertebrate Paleontology & Paleoanthropology, Chinese Academy of Sciences, PO Box 643, Beijing 100044, China

Typescript received 21 July 2020; accepted in revised form 21 December 2020

**Abstract:** Many dinosaurs may have shown ecological differentiation between hatchlings and adults, possibly because of the great size differential. The basal ceratopsian *Psittacosaurus lujiatunensis* is known from thousands of specimens from the Lower Cretaceous of China and these include many so-called ‘juvenile clusters.’ During the early stages of ontogeny, *P. lujiatunensis* underwent a posture shift from quadrupedal to bipedal, and a dietary shift has also been postulated. In this study, we made a 2D mechanical analysis of the jaws of a hatchling and an adult to

determine the differences between the two systems; we found some differences, but these were only modest. The adult was better suited to feeding on tough plant material than the hatchling, based on its higher values of absolute and relative bite forces and higher values of mechanical advantage, but there were no substantial shifts in jaw shape or function.

**Key words:** jaw mechanics, lever system, diet, dietary shift, ceratopsian, Cretaceous.

AMONG large tetrapods, dinosaurs exhibited a remarkably great disparity in size between hatchlings and adults. This is because, while many adults were huge, encompassing the largest creatures ever to walk on land, dinosaur eggs were limited in size by the balance between egg volume and eggshell thickness (Horner 2000). Eggs were rarely larger than an American football, even when adults were 10–50 m long (Carpenter *et al.* 1994), and this means that babies might have hatched and avoided interactions with their parents especially in species with extreme size discrepancy between the newly hatched individuals and adults (Coombs 1982, 1989). The degree of parental care in dinosaurs has been debated (Horner & Makela 1979; Horner 2000; Varricchio 2011) but as their living archosaur relatives, birds and crocodilians, show considerable to modest levels of care for their youngsters at the nest, it is reasonable to assume that dinosaurs shared some of these parental behaviours. Many dinosaurs were precocial, hatching with a full set of teeth and well ossified limbs, ready for action (Norell *et al.* 1995; Horner 1984, 2000) and they may have lived independent lifestyles from their parents.

*Psittacosaurus* is one of the basalmost genera of Ceratopsia; adults lacked the obligate quadrupedality and craniofacial ornamentation of later, derived neoceratopsians. Specimens have been found in the Barremian to

Albian of China, Mongolia and southern Siberia (Osborn 1923; Young 1958; Sereno & Chao 1988; Sereno *et al.* 1988, 2007, 2010; Dong 1993; Russell & Zhao 1996; Averianov *et al.* 2006; Zhou *et al.* 2006; Sereno 2010; Napoli *et al.* 2019). *Psittacosaurus* is unusual in that it comprises many species (19 have been named, of which up to 10 are accepted as valid; Sereno *et al.* 2010; Napoli *et al.* 2019) as well as many specimens, with some species represented by thousands of individuals (Zhao *et al.* 2013a, b). This is why *Psittacosaurus* has been chosen to name a fauna (Dong 1993) and a biochron (Lucas 2006) spanning the Barremian to Albian (129–100 Ma).

*Psittacosaurus lujiatunensis* is one of the most abundantly represented species of the genus, comprising hundreds of specimens located in numerous museums throughout the world. Dozens of juvenile clutches have been reported, especially from the Lujiatun locality in Liaoning Province, where clusters include up to 30 juveniles (Meng *et al.* 2004; Zhao *et al.* 2007; Bo *et al.* 2016). The abundance and quality of the specimens reflect the conditions of their entombment, overwhelmed by falling volcanic ash (Zhao *et al.* 2007, 2013a, b; Erickson *et al.* 2009; Hedrick & Dodson 2013; Rogers *et al.* 2015). The Lujiatun beds are dated from early Barremian to Aptian, with published dates of  $128 \pm 0.2$  Ma, based on

$^{40}\text{Ar}/^{39}\text{Ar}$  dating (Wang *et al.* 2001) or  $123.2 \pm 1.0$  Ma, based on  $^{40}\text{Ar}/^{39}\text{Ar}$  dating (He *et al.* 2006).

Juvenile *Psittacosaurus lujiatunensis* can be aged from their bone histology (Erickson *et al.* 2009, 2015) and in one clutch there were five juveniles aged 2 years and one 3-year old (Zhao *et al.* 2013a). Clusters of young individuals of dinosaurs are rare (Horner & Makela 1979; Forster 1990; Kobayashi & Lü 2003; Varricchio *et al.* 2008a, b; Mathews *et al.* 2009) and, for many specimens of *P. lujiatunensis*, the nature of the deposit suggested that these clusters are evidence for gregarious social behaviour in the juveniles (Zhao *et al.* 2007).

*Psittacosaurus lujiatunensis* underwent a posture shift from quadrupedal to bipedal at about age three to four, as shown by body proportions and estimated growth rates (Zhao *et al.* 2013a). This marked the onset of the exponential phase of growth, when body mass increased rapidly to reach adult values (Erickson *et al.* 2009). The skull accommodated for the shift with a remodelling of its caudal region, a deep modification of the braincase and reduction in the angle of the lateral semicircular canals (Bullar *et al.* 2019) and a general reshaping of the skull from a rounded, almost domed, shape (Fig. 1A–D), typical of the young individuals of many vertebrate species, to a laterally expanded and more angular one (Fig. 1E–H). With growth, there was a positively allometric expansion laterally across the jugals and postorbitals as the snout became narrower (Fig. 1D, H). The orbits became relatively smaller, the lateral temporal fenestrae expanded and the supratemporal fenestrae almost converged mesially, constricting the caudal portion of the

braincase. This remodelling created a marked sagittal crest across the parietals and the caudalmost part of the frontals. These modifications point toward the development of larger and more powerful jaw muscles.

*Psittacosaurus lujiatunensis* had a slicing dentition well suited for the mastication of plant material, and could also have fed on highly fibrous vegetation thanks to gastroliths in the guts of larger individuals (You & Dodson 2004; Sereno *et al.* 2010; Zhao *et al.* 2013b). Gregarious behaviour, juvenile-only clusters and gastroliths in older specimens suggest an ontogenetic dietary shift as well as a postural one (Zhao *et al.* 2013a).

The aim of this paper is to test whether *P. lujiatunensis* underwent an ontogenetic dietary shift based on a biomechanical study of the jaws and teeth of juvenile and adult specimens. We employ a well-tested 2D lever modelling approach to investigate the biomechanics of the mandibles and find differences between the two specimens.

*Institutional abbreviation.* IVPP, Institute of Vertebrate Palaeontology & Palaeoanthropology, Chinese Academy of Science, Beijing, People's Republic of China

## MATERIAL AND METHOD

### Specimens

Two specimens, IVPP V 15451 (Fig. 1A–D) and IVPP V 12617 (Fig. 1E–H), a juvenile and adult, respectively, were

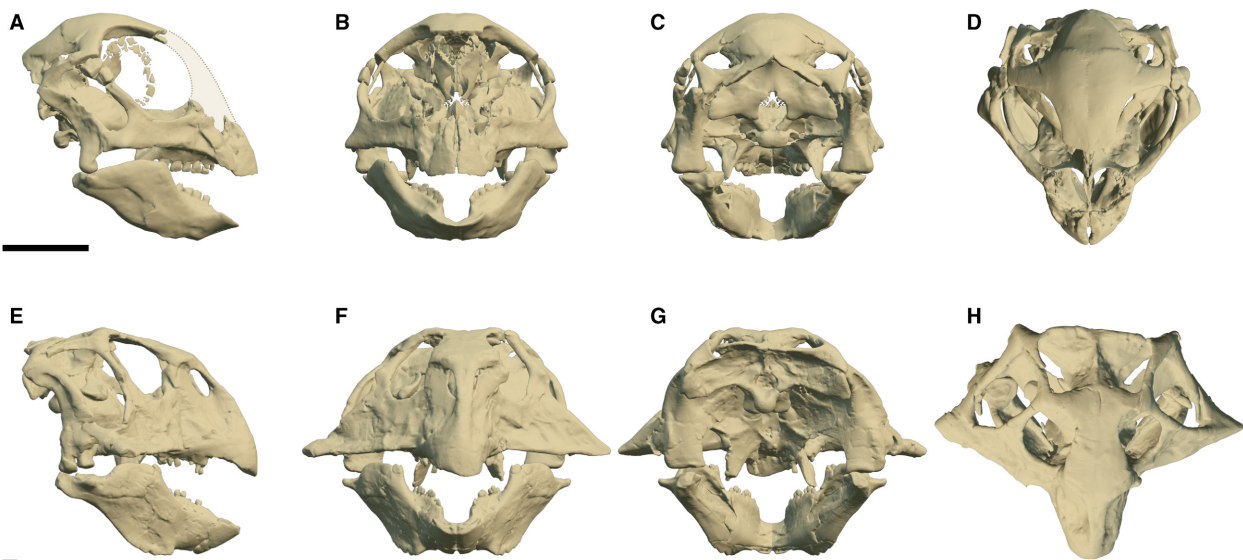


**FIG. 1.** Digitally completed skulls and mandibles. A–D, juvenile specimen IVPP V 15451 in: A, lateral view with dotted area representing the missing skull bones; B, frontal; C, occipital; D, dorsal view. E–H, adult specimen IVPP V 12617 in: E, lateral; F, frontal; G, occipital; H, dorsal view. Scale bars represent 1 cm.

used for this study. Both specimens consist of relatively complete and minimally deformed skulls. IVPP V 12617 was originally described by You & Xu (2005) as the paratype of the new genus and species *Hongshanosaurus houi*, which was later synonymized with *P. lujiatunensis* through the use of 3D geometric morphometrics (Hedrick & Dodson 2013). In the same paper, Hedrick & Dodson (2013) also suggested identity between the species *P. lujiatunensis* and *P. major*, a synonymy first suggested by Erickson *et al.* (2009) on circumstantial evidence, but which was rejected by others (Napoli *et al.* 2019).

The age at death of IVPP V 12617 was calculated by Zhao *et al.* (2013b, 2019) from limb allometry and limb bone histology to be ten years, in other words, an adult individual. IVPP V 15451 was estimated to be a young post-hatchling of less than one year old by its size and the degree of fusion of the bones (Bullar *et al.* 2019). Thus, the specimens represent some of the youngest and oldest individuals of the species known (Zhao *et al.* 2019), constituting end members of an ontogenetic series from an early juvenile stage to adulthood.

Computed tomography (CT) scans of the specimens were provided by IVPP. The CT datasets were made using the Chinese Academy of Sciences micro-computed tomography scanner, on the 450 kV ordinary fossil CT (450-TY-ICT). The scan dataset for IVPP V 12617 consists of 3600 slices with a voxel resolution of 160  $\mu\text{m}$ . The scan dataset for IVPP V 15451 consists of 4302 slices with a voxel resolution of 96.21  $\mu\text{m}$ . The heights and lengths of the entire mandible and its preserved bones for each specimen were measured, the measurements were then normalized to enable direct comparison of function and efficiency of the masticatory apparatus.

#### Digital reconstruction and restoration

The CT data were segmented using Avizo Lite v.9.7.0 (Visualization Sciences Group) to generate virtual models of the two mandibles (Fig. 2). Each mandibular bone was assigned a different label. Both specimens have been modestly taphonomically distorted and are incomplete to various degrees, so reconstructions were made from a hemimandible that exhibited the lowest degree of deformation. The models were then digitally restored using Avizo's mirroring, translation and rotation tools and by filling the many cracks running through the bones (Lautenschlager *et al.* 2016; Lautenschlager 2016) (Fig. 3). In IVPP V 15451 the right hemimandible was chosen for the study as the less deformed, even though it lacks its caudal-most region. To reconstruct the entirety of the hemimandible digitally, the missing parts of the angular and surangular, and the entire articular were then segmented from the undeformed caudal portion of the left

hemimandible. They were then mirrored and carefully placed in their life positions taking advantage of anatomical landmarks and features present on the bone surfaces (Fig. 3A–C). IVPP V 12617 was an almost undeformed specimen and we selected its left hemimandible. While mostly complete, the splenial of IVPP V 12617's right hemimandible was missing. The splenial was segmented and mirrored into position from the left hemimandible (Fig. 3D–F).

#### Mechanical advantage and allometry of the lever system components

*Psittacosaurus*, like other basal ceratopsians but unlike neoceratopsians, does not possess a tooth row extending further back than the coronoid process (Tanoue *et al.* 2009a), making its jaw a third-class lever system. Following Tanoue *et al.* (2009a), we considered the jaw as a two-dimensional lever (Fig. 4), and considered the issues of relative articular offset (Landi *et al.* 2021, fig. S1, table S1), symphyseal length and orientation (Landi *et al.* 2021, figs S2–S3, table S2), and the possibility of skull kinesis (Landi *et al.* 2021, p. 3). It is assumed that the reaction force during the bite produced at the contact with food lies perpendicular to the output lever arm. At equilibrium, when the resultant of all applied forces is zero, such a mechanical system satisfies the general equation:

$$(\text{Total input force}) \times (\text{Input lever}) = (\text{Bite force}) \times (\text{Output lever})$$

thus showing that, to increase the amount of force exerted at the output point while maintaining a constant value for the input force, either the input lever must be lengthened or the output lever must be shortened. By assuming a total input force equivalent to one unit, it is possible to consider the bite force, at any point along the length of the jaw, as a ratio between the input and the output lever:

$$\text{Bite force} = \frac{\text{Input lever}}{\text{Output lever}}$$

This equation provides us with a means to evaluate the mechanical advantage of the bidimensional lever system, that is, its capability to multiply the input force value, its efficiency ( $\eta$ ). The variation in mechanical advantage was then considered at three different points of interest along the mandible: the rostralmost end of the predentary, and the tips of the first and the last tooth of the tooth row. In each case, we chose the largest tooth in the tooth row to represent maximum size (Landi *et al.* 2021, table S3).

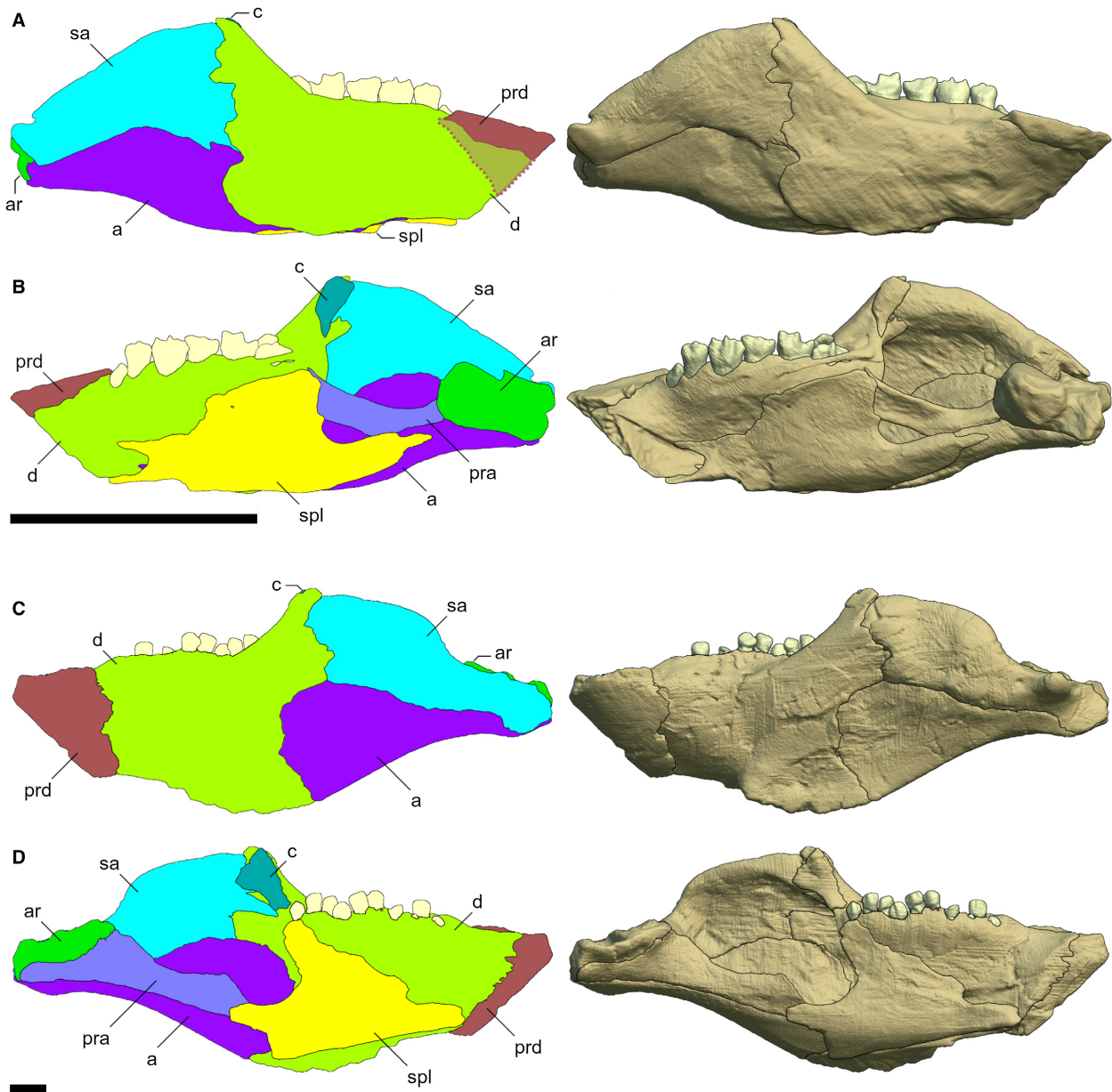


**FIG. 2.** Completed reconstruction of the mandibles of *Psittacosaurus lujiatunensis*. A–B, reconstructed right hemimandible of juvenile specimen IVPP V 15451 in: A, labial view, the area within dashed lines represents the hypothesized complete prementary; B, lingual view. C–D, reconstructed left hemimandible of adult specimen IVPP V 12617 in: C, labial; D, lingual view. *Abbreviations:* a, angular; ar, articular; c, coronoid; d, dentary; pra, prearticular; prd, prementary; sa, surangular; spl, splenial. Scale bars represent 1 cm.

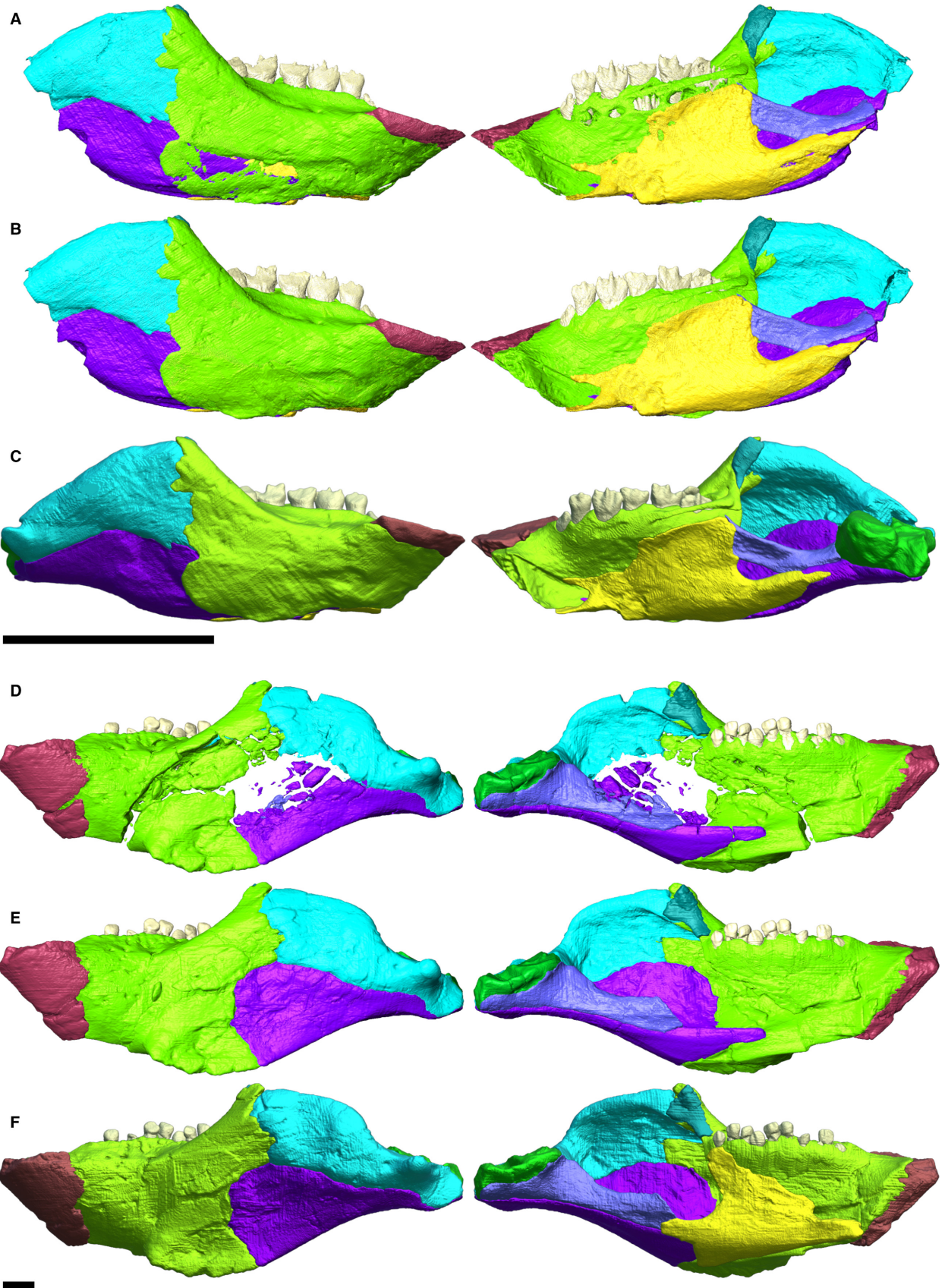
#### *Bite force estimates and muscle placement*

To create an estimate of the muscle input forces for specimen IVPP V15451, we altered the values originally

calculated for IVPP V 12617 by Taylor *et al.* (2017). We downscaled the values assuming isometric growth, using the ratio between the total surface areas of the digitally completed models. Considering the previous 2D lever

**FIG. 3.** Stages of reconstruction and restoration of the mandibles. A–C, juvenile specimen IVPP V15451: A, raw segmentation; B, initial patching and restoration; C, completed reconstruction with restoration of the missing bones. D–F, adult specimen IVPP V 12617: D, initial segmentation; E, initial patching and restoration; F, completed reconstruction with restoration of the missing splenial. Scale bars represent 1 cm.





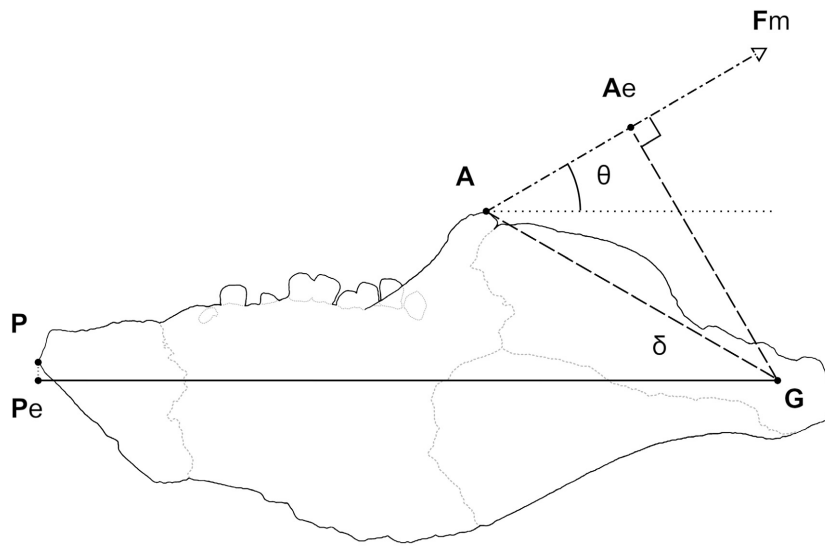


**FIG. 4.** Study of the bite force in *Psittacosaurus lujiatunensis* (after Ostrom 1966), with the points and forces modelled as a second-order lever. Abbreviations: A, apical point of the coronoid process; Ae, intersection point of the effective input lever arm (GAe) for vector  $F_m$ ;  $F_m$ , muscular input force vector, considered as applied onto the point A; G, centre of the glenoid fossa of the articular; P, rostralmost end of the predentary; Pe, projection of point P onto the horizontal line passing through the point G. Line GA, input lever arm; line GPe, output lever arm.

system, the missing factor that could generate differences in bite force is the nature of the adductor muscles, specifically the way the input forces act on the input lever arm and their magnitude. Following Ostrom's (1964, 1966) seminal works, which are widely used (e.g. Mallon & Anderson 2015; Nabavizadeh 2016, 2020a, b), we considered the lever system as seen in Figure 4. In a static equilibrium state, the ceratopsian mandible can be described as follows:

$$F_{\text{bite}} \cdot L_{\text{out-lever}} = F_{\text{muscle}} \cdot [\sin(\delta + \theta) \cdot GA]$$

In the previous equation,  $\sin(\delta + \theta) \cdot GA$  is the length of the effective input lever arm GAe, the perpendicular segment drawn from the point G to the line of action of an input force vector with an angle of attachment  $\theta$ . The line GA, in this model, represents the maximum theoretical length of the input lever arm and so the condition in which the maximum amount of muscular force can be applied to the mechanical system, a condition verified for  $\theta_{\text{max}} = \frac{\pi}{2} - \delta$ . Accordingly, segment GAe will always be shorter than GA. Alternative calculations, based on linear instead of surface measurements (Landi *et al.* 2021, fig. S4, tables S4–S5) differ, but are perhaps less reliable.

In line with similar analyses (Ostrom 1964, 1966; Mallon & Anderson 2015; Nabavizadeh 2016), we considered the musculus adductor mandibulae externus muscle group (MAME) as responsible for most of the applied force on the jaw, and excluded the pterygoideus from consideration. This muscle group, comprising the musculus adductor mandibulae externus profundus (mAMEP), m. adductor mandibulae externus medialis (mAMEM) and m. adductor mandibulae externus superficialis (mAMES), is identified as the main muscle group in bite dynamics and described as almost exclusively responsible for jaw adduction. The vectors of the three muscles

forming MAME were combined to produce a resultant force vector, whose insertion point was placed at the apex of the coronoid process, a practical solution that simplifies the jaw model without exceedingly deviating from the reality of the physical jaw.

To measure the angle of attachment of the muscles and obtain the necessary surface values to downscale the muscle force values, a low-resolution model of both skulls was then created and digitally assembled to match the jaw model (Fig. 5). Accordingly, we estimated the location of the muscle attachment sites directly onto the models using Blender v.2.82a (<https://www.blender.org>). This operation allowed for accurate positioning of the geometric centres of each attachment site in 3D and, accordingly, measurement of the angles of attachment. For all muscles, minimum and maximum estimates for the extent of each muscle attachment's surface area were created following the discernible impressions on the mesh. These are considered as conservative estimates, meant to avoid possible artefacts generated by the segmentation, interpolation and patching procedures performed in Avizo.

As specimen IVPP V 12617 had already been studied by Taylor *et al.* (2017), we employed their work as a reference to locate the position of the muscles and colour code them. We also used Holliday (2009) as a reference for anatomical details concerning muscle placement and osteological correlates for Aves, Crocodylia and Dinosauria. Note that, in two recent publications, Nabavizadeh (2020a, b) described jaw muscle anatomy in ornithischians, including *Psittacosaurus*, with a modified reconstruction of mAMES, inserting down the rostral rim of the coronoid eminence and labial dentary ridge, thereby creating a more rostralabial attachment. A tentative re-run of our analysis based upon this new reconstruction is presented in Landi *et al.* (2021, fig. S5, table S6).

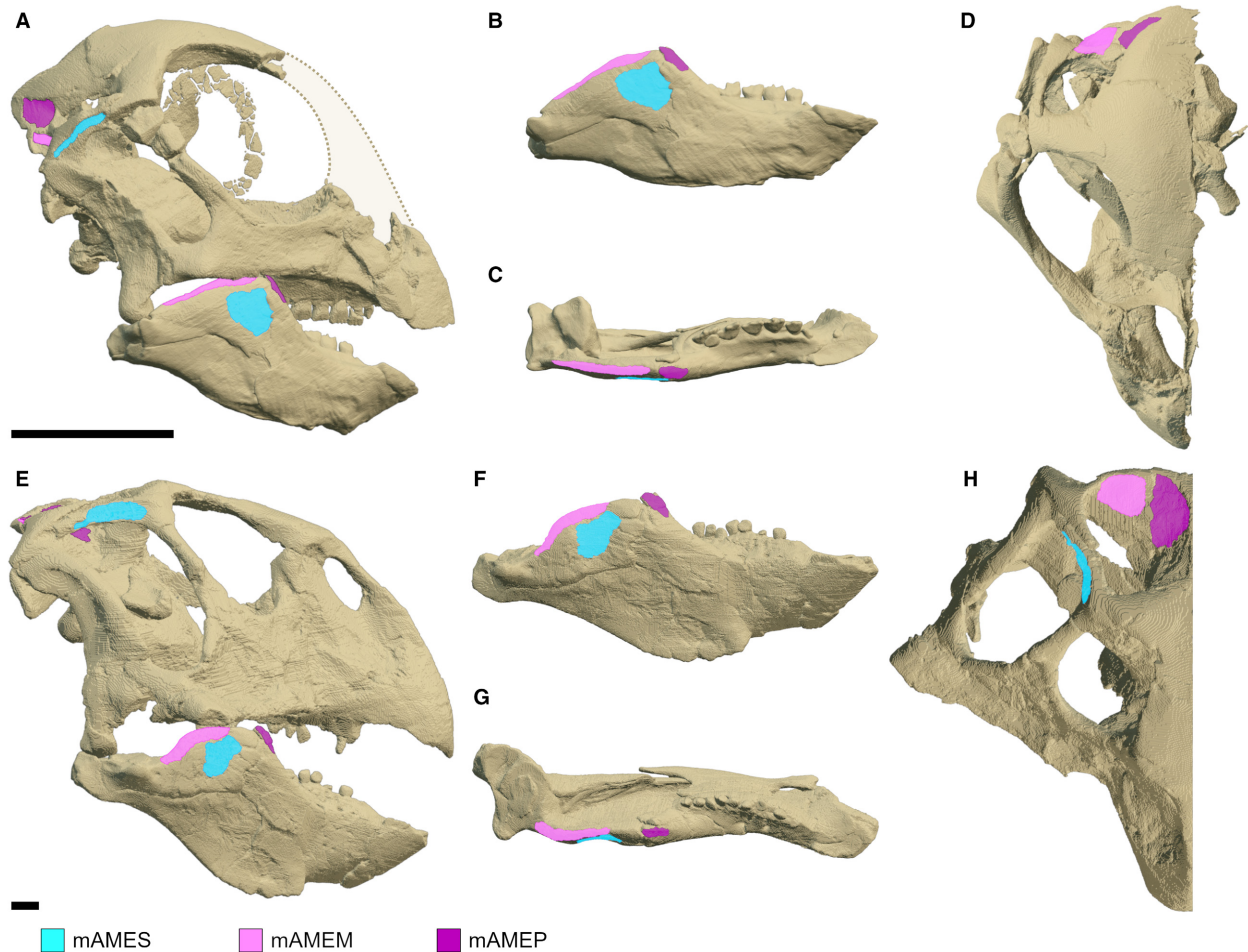


**FIG. 5.** MAME muscle group placement onto the models. A–D, juvenile specimen IVPP V 15451 in: A, composite lateral view, with the area within the dotted lines representing the missing skull bones; B, mandible labial; C, mandible dorsal; D, skull dorsal view. E–H, adult specimen IVPP V 12617 in: E, composite lateral; F, mandible labial; G, mandible dorsal; H, skull dorsal view. Images have been mirrored for illustrative purposes. *Abbreviations:* mAMEM, m. adductor mandibulae externus medialis; mAMEP, m. adductor mandibulae externus profundus; mAMES, m. adductor mandibulae externus superficialis. Scale bars represent 1 cm.

## RESULTS

### *Skeletal element allometry*

The measurements taken and the ratios derived from them are reported in Tables 1–3. During almost ten years of growth, the mandible increased its total length by about 6.36 times and its height by about 6.40 times. Hence, the mandible as a whole, and the dentary (the major osteological component of the mandible) undergo almost perfectly isometric growth through ontogeny. The development of the surangular is almost isometric as well, with a decrease in relative height and length of about 3%, while the angular shortens and lowers. The most remarkable variation is noticeable in the prementary; while its relative length scales in a quasi-isometric fashion, the height of this element is proportionately 23.65% less in IVPP V 15451 than in IVPP V 12617.

Mean lengths for a single tooth and the length of the tooth row are reported in Table 4. On average, a tooth measures 1.35 mm in length in IVPP V 15451 and 4.33 mm in IVPP V 12617; about 3.2 times larger. During ontogeny, the tooth row becomes 5.4 times rostrocaudally longer, an increment also reflecting the increase of the total number of erupted teeth from seven to nine. This absolute increment in size is not quite matched by size increases in other mandibular components, as the tooth row in the adult is 5.24% shorter compared to the whole mandible, and 8.96% compared to the dentary (Table 4). We infer that the total amount of pressure that any force could exert along the tooth row as a whole increased with age. With ontogeny, the distance between the tooth row and the tip of the prementary also increased, creating a diastema on the rostral region of the dentary that is 2.19% relatively longer. In spite of this retrograde movement, the previously discussed concurrent shortening of the tooth row causes its



**TABLE 1.** Length and height values and variations of the mandible and its major components for specimens IVPP V 15451 and IVPP V 12617.

Element	Length (mm)	% Ratio to mandibular length	Height (mm)	% Ratio to mandibular length
<b>IVPP V 15451</b>				
Complete right hemimandible	21.98		9.15	
Predentary (PRD)	4.33	19.72	2.22	24.22
Dentary (D)	12.53	57.02	9.11	99.53
Angular (A)	16.28	74.09	5.39	58.85
Surangular (SA)	11.79	53.66	5.43	59.32
Input lever arm (GA)	8.33	37.91		
Output lever arm (GPe)	20.32	92.45		
<b>IVPP V 12617</b>				
Complete left hemimandible	139.89		58.59	
Predentary (PRD)	27.43	19.61	28.05	47.87
Dentary (D)	79.35	56.72	58.58	99.99
Angular (A)	87.52	62.56	31.42	53.63
Surangular (SA)	79.08	56.53	36.83	62.87
Input lever arm (GA)	56.34	40.27		
Output lever arm (GPe)	129.24	92.39		

caudal end to terminate 3.05% more rostrally compared to IVPP V15451, about the same length as a single tooth.

#### Mechanical advantage

Although the general shape of the jaw, especially in its caudal region, changes through ontogeny, the elements of the lever system appear to be unaltered by such modifications. The efficiency of the two jaw systems is fairly similar, with the adult performing slightly better than the juvenile (Table 5). The angle ( $\delta$ ) between the two lever arms increases from 27.70° to 29.76° (Table 6). The absolute mechanical advantage increases for both specimens moving toward the caudal end of the masticatory system

**TABLE 2.** Percentage variation in length ( $\Delta L$ ) and height ( $\Delta H$ ) of individual bones in specimen IVPP V 12617 compared to IVPP V 15451.

Element	$\Delta L\%$	$\Delta H\%$
Predentary (PRD)	-0.11	23.65
Dentary (D)	-0.3	0.45
Angular (A)	-11.53	-5.22
Surangular (SA)	2.87	3.55

**TABLE 3.** Relationship between cranial and mandibular length in specimens IVPP V 12617 and IVPP V 15451.

Specimen	IVPP V 15451	IVPP V 12617
Mandible length (mm)	21.98	139.89
Skull length (mm)	28.11	156.63
Mandible to skull ratio	78.19%	89.31%

without reaching values of  $\eta \geq 1$ , as expected for a third-class lever system.

The difference in efficiency between the two individuals ( $\Delta\eta$ ), although slight, increases proceeding backwards from the tip of the predentary ( $\Delta\eta$  0.026) to the first tooth ( $\Delta\eta$  0.047). This trend is reversed on moving from the first to the last tooth ( $\Delta\eta$  0.036) of the row.

The values for mechanical advantage that we found are slightly higher than those calculated by Tanoue *et al.* (2009a), but both specimens remain within the maximum and minimum ranges proposed for the Psittacosauridae.

#### Calculated bite force

The calculated input muscle force and output bite force values are reported in Tables 6 and 7. The combined MAME input force in IVPP V 12617 is 30.7 times higher (192.1 N) than in IVPP V 15451 (6.26 N). From our calculations, we estimate a significant increase in the angle of attachment ( $\theta$ ) of the MAME resultant muscle group from 38.23° to 53.94° through ontogeny. This variation allows IVPP V 12617 to transfer the input force to the lever system and closely approaches the system-specific

**TABLE 4.** Values and variations of tooth and tooth row in *Psittacosaurus lujiatunensis*.

	IVPP V 15451	IVPP V 12617
Tooth row length	7.43	39.94
Diastema	3.91	27.96
% proportion of the diastema length relative to the entire mandible	17.80%	19.99%
Rostral end of the tooth row	16.41	101.27
First functional tooth	15.88	94.71
Last functional tooth	9.69	62.93
Caudalmost end of the tooth row	8.97	61.33
% proportion of the caudalmost tooth row point position relative to the entire mandible	40.79%	43.84%
Average tooth length	1.35	4.33
Tooth length relative to the tooth row	18.21%	10.85%
Tooth row length relative to jaw length	33.79%	28.55%
Tooth row length relative to dentary length	59.30%	50.34%

**TABLE 5.** Values and variation of mechanical advantage ( $\eta$ ) for both specimens measured at the tip of the predentary and at the rostralmost and caudalmost tooth.

	IVPP V 15451	IVPP V 12617	Variation	
			$\Delta\eta$	$\Delta\eta\%$
$\eta$ at the tip of the PRD	0.41	0.44	0.03	2.60%
$\eta$ at the first tooth	0.55	0.59	0.05	4.67%
$\eta$ at the last tooth	0.86	0.9	0.04	3.56%

$\theta_{\max}$  value of  $60.24^\circ$ . The output force increases in both mandibles proceeding rostrocaudally, as expected, with the maximum bite force being at the tip of the caudalmost tooth; here, the juvenile is able to generate 4.99 N, 80% of the MAME input force, and the adult 170.15 N, 89% of the muscle force. While with growth the absolute bite force increases by 45.7 times at the tip of the predentary, 46.3 times at the rostralmost tooth and 44.8 times at the caudalmost tooth, the ability of the system to commute the input force into output force increases relative to body size by 5.13%, 7.26% and 8.89% at the same points along the mandible.

## DISCUSSION

The juvenile IVPP V 15451 mandible appears more robust in its caudalmost region, lacking the distinct and elongated tapering we see in the adult IVPP V 12617 and, in fact, the angular was more robust while the surangular was less developed. This probably follows the development of the musculus pterygoideus dorsalis and m. pterygoideus ventralis that attach to the caudoventral region of

**TABLE 6.** Calculated components of the mechanical system for the resultant MAME group and output bite forces at the tip of the predentary, and at the rostralmost and caudalmost tooth.

	IVPP V 15451	IVPP V 12617	Relative percentage variation
Angle $\delta$	27.7	29.76	
Angle $\theta$	38.23	53.94	
Input lever arm (GAe)	7.72	55.74	
MAME group total force (N)	6.26	192.1	
Bite force at the tip of the predentary (N)	2.38	82.85	
Ratio bite force/input force	0.38	0.43	5.13
Bite force at the first tooth (N)	3.04	107.38	
Ratio bite force/input force	0.49	0.56	7.26
Bite force at the last tooth (N)	4.99	170.15	
Ratio bite force/input force	0.8	0.89	8.89

the angular which, consequently, compresses the entire caudal region of the mandible with ontogeny.

Allometric scaling is visible when comparing mandibular length to total skull length, as the mandible becomes relatively longer, representing 78.19% of the total skull length in the juvenile and increasing to 89.31% in the adult (Table 3). As the skull changes from an overall rounder shape to a flatter one with ontogeny, the caudal portion of the skull undergoes important changes linked with both the postural shift and the increased size of the adductor muscles (Bullar *et al.* 2019). More importantly, a sagittal crest forms during ontogeny by the constriction of the parietals and the caudalmost portion of the frontals, a clear indication of the strengthening of the muscles involved in mandibular adduction (Fig. 1H).

Unfortunately, the predentary of the juvenile IVPP V 15451 is incomplete, preserving only part of the dorsal lobe. The supposed ventral lobe extension has been roughly estimated by photographic comparison with individuals from the clutch IVPP V 16902 and the depression left on the surface of the dentary bone of the model (Fig. 2A). This educated guess highlights that the predentary did not envelop the ventral region of the dentary as it does in the adult. This expansion suggests a response to an increased level of stress in the rostral portion of the masticatory apparatus and could be linked to the need to grasp and strip or crush more resistant plant material.

If the two mandibles were the same size, the adult IVPP V 12617 would be better suited for processing food

**TABLE 7.** Muscle force values calculated after isometric downscaling for IVPP V 15451, and original values for IVPP V 12617 (after Taylor *et al.* 2017).

Jaw muscle	IVPP V 15451, Muscle force (N) (after isometric downscaling)	IVPP V 12617, Muscle force (N) (original values)
mAMP	2.29	70.4
mAMEP	1.96	60.1
mAMEM	1.41	43.2
mAMES	2.89	88.8
mPSTs	2.17	66.5
mPTd	0.38	11.6
mPTv	0.66	20.1
mPSM	0.97	29.9
mAMEV	1.39	42.6

*Muscle abbreviations:* mAMEM, m. adductor mandibulae externus medialis; mAMEP, m. adductor mandibulae externus profundus; mAMES, m. adductor mandibulae externus superficialis; mAMEV, m. adductor mandibulae externus ventralis; mAMP, m. adductor mandibulae posterior; mPSM, m. pseudomasseter; mPSTs, m. pseudotemporalis superficialis; mPTd, m. pterygoideus dorsalis; mPTv, pterygoideus ventralis.

because it has a more efficient mechanical lever system for transferring the applied force to different regions of the mandible (Table 5). The increase in the angle of attachment of the MAME group increased the leverage, augmenting the amount of input muscle force effectively transformed to output bite force (Table 6). There is a modest increase in efficiency at the tip of the prementary, indicated by an increase in the relative length of input to output lever arms of 2.60 percentage points in the adult compared to the juvenile (Table 5). The increased diastema (Table 4) allowed for the comparatively higher mechanical advantage and bite force values seen along the tooth row in the adult, IVPP V 12617 (Tables 5, 6). In turn, the shortening of the tooth row relative to the rest of the mandible caused it to terminate in a more rostral position when compared to the juvenile IVPP V 15451 (Table 4); this arrangement generates a lower increase in bite force at the last tooth compared to the first tooth of the row in the adult (Table 6). In a third-class lever system, this retrograde placement of the tooth row implies that it experienced a relatively smaller range of forces whose values were, in any case, higher than in IVPP V15451. Presumably, the higher values estimated for absolute and relative bite forces in the adult IVPP V 12617, coupled with higher values of mechanical advantage, allowed the animal to consume tougher plant material.

Both adult and juvenile *P. lujiatunensis* possess leaf-shaped teeth with self-sharpening cutting edges, well suited for the mastication of plant material (You & Dodson 2004; Tanoue *et al.* 2009b). The shape of the teeth does not appear to vary with ontogeny (Fig. 2), although the mesial carina appears to be taller in IVPP V15451. However, this may simply reflect differences in CT scan resolution, which also hide the secondary ridges of the teeth in IVPP V 12617 (clearly visible in Tanoue *et al.* 2009b, fig. 7D), and the different degree of use and wear of the teeth during growth.

Gastroliths have been reported in various species of *Psittacosaurus*, although they have not been found in adult *P. lujiatunensis* (Osborn 1924; You & Dodson 2004; You & Xu 2005; Wings & Sander 2007; Sereno *et al.* 2010; Napoli *et al.* 2019; Zhao *et al.* 2019). It is assumed that such stones found in the thoracic cavity, identified as true gastroliths, would have helped the animal in processing food by creating a gastric mill (Wings 2007; Wings & Sander 2007; Fritz *et al.* 2011; Sereno *et al.* 2010). If the adults had gastroliths, this could explain why they did not show increases in relative mechanical advantage and bite force. By comparison with birds, as their closest living relatives, it is plausible that *Psittacosaurus* juveniles might have employed gastroliths as well, because many bird species such as pheasants, sparrows, tits and grouse (Harper 1964; Wings 2007) that use gastroliths as adults begin using them as juveniles. According to Wings

(2007), the expected diameter of the gastroliths in such young individuals would roughly match that of the encasing sediment clasts, and so they could be hard to recognize in the specimens.

Even though the mandible underwent an apparent general reshaping through ontogeny (Fig. 2) the components of the lever system remained strongly conservative in their size relative to the entire mandible, resulting in mechanical advantage remaining minimally altered through ontogeny. A shift in diet, while not uncommon in modern reptiles such as squamates (Vincent *et al.* 2007) and crocodilians (Erickson *et al.* 2003), as well as inferred in dinosaurs (Bailleul *et al.* 2016; Woodruff *et al.* 2018; Frederickson *et al.* 2020), need not be directly correlated to morphological changes through ontogeny. Extant taxa that show a shift in diet show a variety of morphological changes: allometric changes in head shape, variation of intrinsic muscle properties, changes in mass and/or geometry of the adductor muscles, and augmentation of the mechanical advantage of the system (Herrel *et al.* 2002; Anderson *et al.* 2008). Durophagy, the pathway suggested for *Psittacosaurus* (Sereno *et al.* 2010), is generally associated with the development of stronger bites, especially in the caudal portion of the toothrow. Usually, durophagous taxa show a considerable allometric increase in bite force relative to changes in measures of head and body (Pfaller *et al.* 2010a). One example is *Varanus niloticus* (Rieppel & Labhardt 1979), which shifts diet from insectivory in juveniles to molluscivory in adults. Adults have a toothrow which is relatively shorter than that of the juveniles, complemented by the development of a set of more massive teeth at the caudal end. This modification has been interpreted as a means to reduce the average distance between the point of application of the muscle force and the bite point, generating a stronger bite without the need for greater muscle force compared to same-size related species. As discussed before, the mechanical system of *P. lujiatunensis* undergoes an analogous reduction in the length of the toothrow. A different example of ontogenetic adaptation to durophagy is provided by another beaked reptile, the turtle *Stenothemus minor* (Herrel & O'Reilly 2006; Pfaller *et al.* 2010a, b). The adults of this species achieve a greater bite force by modifying their head morphology and musculature instead of the jaw lever system. The adductor musculature becomes more massive, with a more efficient muscle architecture. At the same time, the cranium develops in a positive allometric fashion relative to the carapace to accommodate the larger musculature, a condition that goes against the general trend in vertebrates in which the head shows negative allometry with growth.

In *Psittacosaurus*, the adult, being larger, shows absolute bite force values that are up to 46 times stronger than those of the juvenile. This arises from a combination of increased muscular force with increased size, reshaping

of the skull that moved the insertion points of the individual MAME group muscles to give them a higher angle of attachment, and increased length of the diastema. Such modifications led to higher relative bite force values with ontogeny. While our model employs a simple isometric scaling of the muscle force, we can speculate that, as the mechanical system grew more efficient and the bite force relatively higher, enlargement of the adductor fossa in the adult, coupled with the formation of a sagittal crest, could have accommodated an adductor musculature disproportionately larger than in the juvenile (Figs 1D, H, 5D, H). The potential presence of gastroliths in adults and a complete dentition could have made them able to process their food even more efficiently. In fact, the co-occurrence of gastroliths and a fully developed masticatory system is an uncommon, almost unique, feature, only seen in *Psittacosaurus* and *Gasparinisaura*, and possibly in *Yinlong*, and would have enabled these animals to consume tougher plant material (Wings & Sander 2007; Cerda 2008; Fritz *et al.* 2011). Putting these lines of evidence together, adult *Psittacosaurus* were better equipped for processing food, being able to feed on a wider range of plant material including tougher fodder than the juveniles (Ostrom 1966; Sereno *et al.* 2010; Maiorino *et al.* 2018). We cannot say when the dietary shift occurred, and it is yet to be established whether it coincided with the onset of the postural shift and the exponential phase of growth.

Nesting behaviour in ceratopsians is debated because specimens of nesting structures, eggs or newly hatched juveniles are rare (Brown & Schlaikjer 1940; Horner 1982; Fastovsky *et al.* 2011; Hedrick & Dodson 2013), a preservation bias possibly reflecting the non-biomineralized egg-shell in basal members of the clade (Norell *et al.* 2020). The previously supposed nest of *Psittacosaurus*, reported by Meng *et al.* (2004), is, in fact, a carefully crafted hoax (Zhao *et al.* 2013b). Our evidence supports the idea of precocial hatchlings in *Psittacosaurus lujiatunensis* already postulated for other members of the genus (Coombs 1980). With parental care being unlikely, the young dinosaurs, once hatched would have abandoned the nest and formed 'sibling groups' or 'pod formations' (Coombs 1982, 1989), gathering together by cohort for protection, as in some extant archosaurs. Adult *P. lujiatunensis* developed a jaw-cranial complex that seems to broaden its foraging spectrum, moving to tougher fodder. We can assume that these changes in maximum bite force would have acted to reduce the competition between juvenile and adult individuals of the same species, as seen in some living reptiles (Herrel & O'Reilly 2006; Anderson *et al.* 2008). The smaller body size, weaker masticatory system, with less effective lever mechanics and an overall weaker bite, and the absence of post-oral processing structures would have forced the

hatchlings to feed upon different, softer, plant material with modest or no overlap with adults.

#### *Critique of our methods*

*Possible errors in reconstruction.* The process of reconstruction by the juxtaposition of the IVPP V 15451 mandible was conducted with the utmost care. Despite this, we have reservations concerning deformation of the jaw. In particular, the angular and surangular appear to have been pushed mesially, leaving a small gap between their labial surfaces and the lingual one of the dentary along the main suture line. Moreover, the restored area in the IVPP V 15451 model might have masked the correct placement of the centre of the glenoid fossa. The articular comprised three masses of bone not yet completely ossified and was crushed by a rogue bone splinter, possibly part of the labial surface of the surangular. While the patching process joined the bone masses, it also covered most of the depression left by the splinter leaving the glenoid fossa enlarged by some unknown extent, as it was most probably lodged within that same depression. Despite our concerns, all these possible deformations and uncertainty factors were deemed to be acceptable.

In terms of reconstruction of the muscle placements on the bones, the juvenile IVPP V15451, as expected, showed only faint osteological markers, and some might have been missed despite careful comparison with the adult and with published accounts. Further, the numerous bone splinters of the dentary, angular and surangular, which could be pieced together in the reconstruction process, doubtless also concealed some of the indicators of muscle attachment.

In line with earlier authors (Ostrom 1964, 1966; Mallon & Anderson 2015; Nabavizadeh 2016), we did not consider the pterygoideus muscle in our estimates of jaw muscle forces. As Nabavizadeh (2016, p. 291) noted, the pterygoideus is a major contributor to jaw closure in living crocodilians, birds and lizards, and is likely to have been variable in size in ornithischians; contributing to occlusion, mediolateral translation, restriction, and possibly long-axis rotation of the mandible. However, as those previous authors did, we excluded the pterygoideus from our calculations as it is difficult to estimate the vertical vector of those forces that would contribute to jaw closure, and those forces are in any case likely to be considerably less than the sum of the adductor muscles (Table 7).

*Scaling sources of error.* Our choice to downscale the muscles using an isometric approach might have introduced a simplification of reality. If, for example, muscle forces in *Psittacosaurus* scaled with positive allometry through ontogeny as in *Alligator mississippiensis* (Gignac



& Erickson 2016), we have slightly overestimated values in IVPP V15451.

**Angular measurement uncertainty.** While most measures, taken with ImageJ v.1.53a, are deemed highly accurate (relative error < 0.5%), those for the angle of attachment of the muscles have the highest uncertainty. While still reasonably precise, the angles for IVPP V 15451 tend to be less accurate. This is due to the slight deformation of the cranium, specifically the mesial movement of the squamosal bone accompanied by the absence of the medioventral portion of the parietal. Although we attempted to reconstruct and place them in the correct anatomical positions, the cranial anchorage sites for mAMES and mAMEP remain partially unresolved, both lacking their natural rostral edges.

## CONCLUSION

We found biomechanical differences between the jaws of juvenile and adult *Psittacosaurus*, as expected, although less substantial than what we might have expected if there had been a major shift in diet to match the posture shift that occurred when individuals were three to four years old. We did find that the jaws of adult *Psittacosaurus lujiatunensis* were relatively more powerful than those of the juvenile. The modifications that contribute to this increase in force indicate that adult *Psittacosaurus* could feed on tougher vegetation than the juveniles, and that could have been enhanced if the adults had gastroliths.

**Acknowledgements.** We thank Yun Feng for making the CT scans of both specimens at IVPP, and Liz Martin-Silverstone and Antonio Balle Mayoral for assistance and discussions. We also thank referees Andrew Farke and Ali Nabavizadeh, editors Laura Porro and Sally Thomas for all their help in improving the manuscript.

## DATA ARCHIVING STATEMENT

Data for this study are available in the Dryad Digital Repository: <https://doi.org/10.5061/dryad.6hdr7sqzk>. Original scan data (data sets IVPP V 15451.CT01 and IVPP V 12617.CT01 for the specimens with the same respective prefixes) are available by request from the Collection House of IVPP: [bbg@ivpp.ac.cn](mailto:bbg@ivpp.ac.cn).

Editor. Laura Porro

## REFERENCES

ANDERSON, R. A., McBRAYER, L. D. and HERREL, A. 2008. Bite force in vertebrates: opportunities and caveats for

- use of a nonpareil whole-animal performance measure. *Biological Journal of the Linnean Society*, **93**, 709–720.
- AVERIANOV, A. O., VORONKEVICH, A. V., LESHCHINSKIY, S. V. and FAYNGERTZ, A. V. 2006. A ceratopsian dinosaur *Psittacosaurus sibiricus* from the Early Cretaceous of West Siberia, Russia and its phylogenetic relationships. *Journal of Systematic Palaeontology*, **4**, 359–395.
- BAILLEUL, A. M., SCANNELLA, J. B., HORNER, J. R. and EVANS, D. C. 2016. Fusion patterns in the skulls of modern archosaurs reveal that sutures are ambiguous maturity indicators for the Dinosauria. *PLoS One*, **11**, e0147687.
- BO, Z., HEDRICK, B. P., CHUNLING, G., TUMARKIN-DERATZIAN, A. R., FENGJIAO, Z., CAIZHI, S. and DODSON, P. 2016. Histologic examination of an assemblage of *Psittacosaurus* (Dinosauria: Ceratopsia) juveniles from the Yixian formation (Liaoning, China): juvenile *Psittacosaurus* histology. *The Anatomical Record*, **299**, 601–612.
- BROWN, B. and SCHLAIKER, E. M. 1940. The structure and relationships of *Protoceratops*. *Transactions of the New York Academy of Sciences*, **2**, 99–100.
- BULLAR, C. M., ZHAO, Q., BENTON, M. J. and RYAN, M. J. 2019. Ontogenetic braincase development in *Psittacosaurus lujiatunensis* (Dinosauria: Ceratopsia) using micro-computed tomography. *PeerJ*, **7**, e7217.
- CARPENTER, K., HIRSCH, K. F. and HORNER, J. R. 1994. *Dinosaur eggs and babies*. Cambridge University Press, 372 pp.
- CERDA, I. A. 2008. Gastroliths in an ornithomimid dinosaur. *Acta Palaeontologica Polonica*, **53**, 351–355.
- COOMBS, W. P. 1980. Juvenile ceratopsians from Mongolia—the smallest known dinosaur specimens. *Nature*, **283**, 380–381.
- 1982. Juvenile specimens of the ornithischian dinosaur *Psittacosaurus*. *Palaeontology*, **25**, 89–107.
- 1989. Modern analogs for dinosaur nesting and parental behavior. *Geological Society of America Special Paper*, **238**, 21–53.
- DONG, Z.-M. 1993. Early Cretaceous dinosaur faunas in China: an introduction. *Canadian Journal of Earth Sciences*, **30**, 2096–2100.
- ERICKSON, G. M., LAPPIN, A. K. and VLIET, K. A. 2003. The ontogeny of bite-force performance in American alligator (*Alligator mississippiensis*). *Journal of Zoology*, **260**, 317–327.
- MAKOVICKY, P. J., INOUE, B. D., ZHOU, C.-F. and GAO, K.-Q. 2009. A life table for *Psittacosaurus lujiatunensis*: initial insights into ornithischian dinosaur population biology. *The Anatomical Record*, **292**, 1514–1521.
- — — — — 2015. Flawed analysis? A response to Myhrvold. *The Anatomical Record*, **298**, 1669–1672.
- FASTOVSKY, D. E., WEISHAMPEL, D. B., WATABE, M., BARSBOLD, R., TSOGTBAATAR, K. and NARMAN-DAKH, P. 2011. A nest of *Protoceratops andrewsi* (Dinosauria, Ornithischia). *Journal of Paleontology*, **85**, 1035–1041.
- FORSTER, C. A. 1990. Evidence for juvenile groups in the ornithomimid dinosaur *Tenontosaurus tilletti* Ostrom. *Journal of Paleontology*, **64**, 164–165.
- FREDERICKSON, J. A., ENGEL, M. H. and CIFELLI, R. L. 2020. Ontogenetic dietary shifts in *Deinonychus antirrhopus* (Theropoda; Dromaeosauridae): insights into the ecology and

- social behavior of raptorial dinosaurs through stable isotope analysis. *Palaeogeography, Palaeoclimatology, Palaeoecology*, **552**, 109780.
- FRITZ, J., HUMMEL, J., KIENZLE, E., WINGS, O., STREICH, W. J. and CLAUSS, M. 2011. Gizzard vs. teeth, it's a tie: food-processing efficiency in herbivorous birds and mammals and implications for dinosaur feeding strategies. *Paleobiology*, **37**, 577–586.
- GIGNAC, P. M. and ERICKSON, G. M. 2016. Ontogenetic bite-force modeling of *Alligator mississippiensis*: implications for dietary transitions in a large-bodied vertebrate and the evolution of crocodylian feeding. *Journal of Zoology*, **299**, 229–238.
- HARPER, J. A. 1964. Calcium in grit consumed by hen pheasants in east-central Illinois. *Journal of Wildlife Management*, **28**, 264–270.
- HE, H. Y., WANG, X. L., ZHOU, Z. H., JIN, F., WANG, F., YANG, L. K., DING, X., BOVEN, A. and ZHU, R. X. 2006.  $^{40}\text{Ar}/^{39}\text{Ar}$  dating of Lujiatun Bed (Jehol Group) in Liaoning, northeastern China. *Geophysical Research Letters*, **33**, L04303.
- HEDRICK, B. P. and DODSON, P. 2013. Lujiatun psittacosaurids: understanding individual and taphonomic variation using 3D geometric morphometrics. *PLoS One*, **8**, e69265.
- HERREL, A. and O'REILLY, J. C. 2006. Ontogenetic scaling of bite force in lizards and turtles. *Physiological & Biochemical Zoology*, **79**, 31–42.
- and RICHMOND, A. M. 2002. Evolution of bite performance in turtles. *Journal of Evolutionary Biology*, **15**, 1083–1094.
- HOLLIDAY, C. M. 2009. New insights into dinosaur jaw muscle anatomy. *The Anatomical Record*, **292**, 1246–1265.
- HORNER, J. R. 1982. Evidence of colonial nesting and 'site fidelity' among ornithischian dinosaurs. *Nature*, **297**, 675–676.
- 1984. The nesting behavior of dinosaurs. *Scientific American*, **250**, 130–137.
- 2000. Dinosaur reproduction and parenting. *Annual Review of Earth & Planetary Sciences*, **28**, 19–45.
- and MAKELA, R. 1979. Nest of juveniles provides evidence of family structure among dinosaurs. *Nature*, **282**, 296–298.
- KOBAYASHI, Y. and LÜ, J.-C. 2003. A new ornithomimid dinosaur with gregarious habits from the Late Cretaceous of China. *Acta Palaeontologica Polonica*, **48**, 235–259.
- LANDI, D., KING, L., ZHAO, Q., RAYFIELD, E. J. and BENTON, M. J. 2021. Supplementary material for: "Testing for a dietary shift in the Early Cretaceous ceratopsian dinosaur *Psittacosaurus lujiatunensis*". *Dryad Digital Repository*. <https://doi.org/10.5061/dryad.6hnr7sqzk>
- LAUTENSCHLAGER, S. 2016. Reconstructing the past: methods and techniques for the digital restoration of fossils. *Royal Society Open Science*, **3**, 160342.
- BRASSEY, C. A., BUTTON, D. J. and BARRETT, P. M. 2016. Decoupled form and function in disparate herbivorous dinosaur clades. *Scientific Reports*, **6**, 26495.
- LUCAS, S. G. 2006. The *Psittacosaurus* biochron, Early Cretaceous of Asia. *Cretaceous Research*, **27**, 189–198.
- MAIORINO, L., FARKE, A. A., KOTSAKIS, T., RAIA, P. and PIRAS, P. 2018. Who is the most stressed? Morphological disparity and mechanical behavior of the feeding apparatus of ceratopsian dinosaurs (Ornithischia, Marginocephalia). *Cretaceous Research*, **84**, 483–500.
- MALLON, J. C. and ANDERSON, J. S. 2015. Jaw mechanics and evolutionary paleoecology of the megaherbivorous dinosaurs from the Dinosaur Park Formation (upper Campanian) of Alberta, Canada. *Journal of Vertebrate Paleontology*, **35**, e904323.
- MATHEWS, J. C., BRUSATTE, S. L., WILLIAMS, S. A. and HENDERSON, M. D. 2009. The first *Triceratops* bonebed and its implications for gregarious behavior. *Journal of Vertebrate Paleontology*, **29**, 286–290.
- MENG, Q., LIU, J., VARRICCHIO, D. J., HUANG, T. and GAO, C. 2004. Parental care in an ornithischian dinosaur. *Nature*, **431**, 145–146.
- NABAVIZADEH, A. 2016. Evolutionary trends in the jaw adductor mechanics of ornithischian dinosaurs: jaw mechanics in ornithischian dinosaurs. *The Anatomical Record*, **299**, 271–294.
- 2020a. New reconstruction of cranial musculature in ornithischian dinosaurs: implications for feeding mechanisms and buccal anatomy. *The Anatomical Record*, **303**, 347–362.
- 2020b. Cranial musculature in herbivorous dinosaurs: a survey of reconstructed anatomical diversity and feeding mechanisms. *The Anatomical Record*, **303**, 1104–1145.
- NAPOLI, J. G., HUNT, T., ERICKSON, G. M. and NORELL, M. A. 2019. *Psittacosaurus amitabha*, a new species of ceratopsian dinosaur from the Ondai Sayr Locality, Central Mongolia. *American Museum Novitates*, **2019**, 1–36.
- NORELL, M. A., CLARK, J. M., CHIAPPE, L. M. and DASHZEVEG, D. 1995. A nesting dinosaur. *Nature*, **378**, 774–776.
- WIEMANN, J., FABBRI, M., YU, C., MARSI-CANO, C. A., MOORE-NALL, A., VARRICCHIO, D. J., POL, D. and ZELENIISKY, D. K. 2020. The first dinosaur egg was soft. *Nature*, **583**, 406–410.
- OSBORN, H. F. 1923. Two Lower Cretaceous dinosaurs of Mongolia. *American Museum Novitates*, **95**, 1–10.
- 1924. *Psittacosaurus* and *Protiguanodon*: two Lower Cretaceous iguanodonts from Mongolia. *American Museum Novitates*, **127**, 1–16.
- OSTROM, J. H. 1964. A functional analysis of jaw mechanics in the dinosaur *Triceratops*. *Postilla*, **88**, 1–35.
- 1966. Functional morphology and evolution of the ceratopsian dinosaurs. *Evolution*, **20**, 290–308.
- PFALLER, J. B., GIGNAC, P. M. and ERICKSON, G. M. 2010a. Ontogenetic changes in jaw-muscle architecture facilitate durophagy in the turtle *Sternotherus minor*. *Journal of Experimental Biology*, **214**, 1655–1667.
- HERRERA, N. D., GIGNAC, P. M. and ERICKSON, G. M. 2010b. Ontogenetic scaling of cranial morphology and bite-force generation in the loggerhead musk turtle. *Journal of Zoology*, **280**, 280–289.
- RIEPEL, O. and LABHARDT, L. 1979. Mandibular mechanics in *Varanus niloticus* (Reptilia: Lacertilia). *Herpetologica*, **32**, 158–163.
- ROGERS, C. S., HONE, D. W. E., McNAMARA, M. E., ZHAO, Q., ORR, P. J., KEARNS, S. L. and BENTON, M. J. 2015. The Chinese Pompeii? Death and destruction of dinosaurs in the Early Cretaceous of Lujiatun, NE China. *Palaeogeography, Palaeoclimatology, Palaeoecology*, **427**, 89–99.

- RUSSELL, D. A. and ZHAO, X.-J. 1996. New psittacosaur occurrences in Inner Mongolia. *Canadian Journal of Earth Sciences*, **33**, 637–648.
- SERENO, P. C. 2010. Taxonomy, cranial morphology, and relationships of parrot-beaked dinosaurs (Ceratopsia: *Psittacosaurus*). 21–58. In RYAN, M. J., CHINNERY-ALLGIER, B. J. and EBERTH, D. A. (eds). *New perspectives on horned dinosaurs: The Royal Tyrrell Museum Ceratopsian Symposium*. Indiana University Press, 623 pp.
- and CHAO, S. 1988. *Psittacosaurus xinjiangensis* (Ornithischia: Ceratopsia), a new psittacosaur from the Lower Cretaceous of Northwestern China. *Journal of Vertebrate Paleontology*, **8**, 353–365.
- SHICHIN, C., ZHENGWU, C. and CHENGANG, R. 1988. *Psittacosaurus meileyingensis* (Ornithischia: Ceratopsia), a new psittacosaur from the Lower Cretaceous of north-eastern China. *Journal of Vertebrate Paleontology*, **8**, 366–377.
- XIJIN, Z., BROWN, L. and LIN, T. 2007. New psittacosaurid highlights skull enlargement in horned dinosaurs. *Acta Palaeontologica Polonica*, **52**, 275–284.
- — and LIN T. 2010. A new psittacosaur from Inner Mongolia and the parrot-like structure and function of the psittacosaur skull. *Proceedings of the Royal Society B*, **277**, 199–209.
- TANOUE, K., GRANDSTAFF, B. S., YOU, H.-L. and DODSON, P. 2009a. Jaw mechanics in basal Ceratopsia (Ornithischia, Dinosauria). *The Anatomical Record*, **292**, 1352–1369.
- YOU, H.-L. and DODSON, P. 2009b. Comparative anatomy of selected basal ceratopsian dentitions. *Canadian Journal of Earth Sciences*, **46**, 425–439.
- TAYLOR, A. C., LAUTENSCHLAGER, S., QI, Z. and RAYFIELD, E. J. 2017. Biomechanical evaluation of different musculoskeletal arrangements in *Psittacosaurus* and implications for cranial function: muscle arrangement in *Psittacosaurus*. *The Anatomical Record*, **300**, 49–61.
- VARRICCHIO, D. J. 2011. A distinct dinosaur life history? *Historical Biology*, **23**, 91–107.
- MOORE, J. R., ERICKSON, G. M., NORELL, M. A., JACKSON, F. D. and BORKOWSKI, J. J. 2008a. Avian paternal care had dinosaur origin. *Science*, **322**, 1826–1828.
- SERENO, P. C., XIJIN, Z., LIN, T., WILSON, J. A. and LYON, G. H. 2008b. Mud-trapped herd captures evidence of distinctive dinosaur sociality. *Acta Palaeontologica Polonica*, **53**, 567–578.
- VINCENT, S. E., MOON, B. R., HERREL, A. and KLEY, N. J. 2007. Are ontogenetic shifts in diet linked to shifts in feeding mechanics? Scaling of the feeding apparatus in the banded watersnake *Nerodia fasciata*. *Journal of Experimental Biology*, **210**, 2057–2068.
- WANG, S. S., HU, H. G., LI, P. X., WANG, Y. Q. and WANG, S. S. 2001. Further discussion on the geologic age of Sihetun vertebrate assemblage in western Liaoning, China: evidence from Ar-Ar dating. *Acta Petrologica Sinica*, **17**, 663–668.
- WINGS, O. 2007. A review of gastrolith function with implications for fossil vertebrates and a revised classification. *Acta Palaeontologica Polonica*, **52**, 1–16.
- and SANDER, P. M. 2007. No gastric mill in sauropod dinosaurs: new evidence from analysis of gastrolith mass and function in ostriches. *Proceedings of the Royal Society B*, **274**, 635–640.
- WOODRUFF, D. C., CARR, T. D., STORRS, G. W., WASKOW, K., SCANNELLA, J. B., NORDÉN, K. K. and WILSON, J. P. 2018. The smallest diplodocid skull reveals cranial ontogeny and growth-related dietary changes in the largest dinosaurs. *Scientific Reports*, **8**, 14341.
- YOU, H. L. and DODSON, P. 2004. Basal Ceratopsia. 478–493. In WEISHAMPEL, D. (ed.) *The Dinosauria*. University of California Press, 880 pp.
- and XU, X. 2005. An adult specimen of *Hongshanosaurus houi* (Dinosauria: Psittacosauridae) from the Lower Cretaceous of Western Liaoning Province, China. *Acta Geologica Sinica*, **79**, 168–173.
- YOUNG, C. C. 1958. The dinosaurian remains of Laiyang, Shantung. *Palaeontologica Sinica*, **142 C**, 1–138.
- ZHAO, Q., BARRETT, P. M. and EBERTH, D. A. 2007. Social behaviour and mass mortality in the basal ceratopsian dinosaur *Psittacosaurus* (Early Cretaceous, People's Republic of China): social behaviour and mass mortality in ceratopsian dinosaur. *Palaeontology*, **50**, 1023–1029.
- BENTON, M. J., SULLIVAN, C., MARTIN SANDER, P. and XU, X. 2013a. Histology and postural change during the growth of the ceratopsian dinosaur *Psittacosaurus lujiatunensis*. *Nature Communications*, **4**, 2079.
- — XU, X. and SANDER, P. M. 2013b. Juvenile-only clusters and behaviour of the Early Cretaceous dinosaur *Psittacosaurus*. *Acta Palaeontologica Polonica*, **59**, 827–833.
- — HAYASHI, S. and XU, X. 2019. Ontogenetic stages of ceratopsian dinosaur *Psittacosaurus* in bone histology. *Acta Palaeontologica Polonica*, **64**, 323–334.
- ZHOU, C.-F., GAO, K.-Q., FOX, R. C. and CHEN, S.-H. 2006. A new species of *Psittacosaurus* (Dinosauria: Ceratopsia) from the Early Cretaceous Yixian formation, Liaoning, China. *Palaeoworld*, **15**, 100–114.